Breakdown coefficients and scaling properties of rain fields

D. Harris, M. Menabde, A. Seed, G. Austin

Nonlinear Processes in Geophysics (1998) 5: 93–104

Nonlinear Processes in Geophysics

Breakdown coefficients and scaling properties of rain fields

D. Harris, M. Menabde, A. Seed* and G. Austin

Department of Physics, University of Auckland, Private Bag 92019, Auckland, New Zealand
*new affiliation: Hydrology Division, Bureau of Meteorology, GPO Box 1289 K, Melbourne, Victoria 3001, Australia

Received: 29 September 1997 – Accepted: 11 August 1998

Abstract. The theory of scale similarity and breakdown coefficients is applied here to intermittent rainfall data consisting of time series and spatial rain fields. The probability distributions (pdf) of the logarithm of the breakdown coefficients are the principal descriptor used. Rain fields are distinguished as being either multiscaling or multiaffine depending on whether the pdfs of breakdown coefficients are scale similar or scale dependent, respectively. Parameter estimation techniques are developed which are applicable to both multiscaling and multiaffine fields. The scale parameter (width), σ, of the pdfs of the log-breakdown coefficients is a measure of the intermittency of a field. For multiaffine fields, this scale parameter is found to increase with scale in a power-law fashion consistent with a bounded-cascade picture of rainfall modeling. The resulting power-law exponent, H, is indicative of the smoothness of the field. Some details of breakdown coefficient analysis are addressed and a theoretical link between this analysis and moment scaling analysis is also presented. Breakdown coefficient properties of cascades are also investigated in the context of parameter estimation for modeling purposes.

1 Introduction

Rainfall is one of many geophysical fields displaying variability over a wide range of scales. Recent methods in the analysis of such fields rely on the self-similar or scaling properties of these fields. The multifractal and multiscaling framework for characterizing rainfall and other geophysical fields has been actively developed over the last decade (see Foufoula-Georgiou and Krajewski (1995) and Lovejoy and Schertzer (1995) for reviews of applications of multifractals to rainfall). To a certain extent, much of the theory for multiscaling originates from the study of turbulence where one aims to describe the scaling properties of velocity fluctuations in a turbulent field. The picture of hydrodynamical turbulence as a cascade of energy from large to small scales, resulting in the scaling properties of the velocity fluctuations, has played an important role in the theory of turbulence. An approach based on the theory of self-similar random fields has been developed largely by Novikov since the late 1960's and is known as scale similarity (Novikov, 1990, 1994; Pedrizzetti et al., 1996 and references therein). Scale similarity is focused on quantities called breakdown coefficients (BDCs) which are defined as the ratio of values of a random field averaged over different scales where the smaller is contained within the larger. In other words, consider a D-dimensional field, $F(\vec{r})$, which is non-negative and on which one defines a local density or average also dependent on $\vec{r}$,

$$F_l(\vec{r}) = \frac{1}{l^D} \int_{V_l} F(\vec{r}\,') d^D r' \tag{1}$$

where V_l is a cube centered at $\vec{r}$. With densities defined at two scales, l and L, the BDC is defined (Novikov, 1990, 1994) by

$$a_{l;L} = F_l(\vec{r}\,^*) / F_L(\vec{r}), \quad l > L, \tag{2}$$

where $\vec{r}$ and $\vec{r}\,^*$ may be different but within the same volume (i.e., $V_l \subset V_L$).

Scale similarity analysis or BDC analysis involves computing BDCs and characterizing their distributions. In this work BDC analysis is performed using rainfall data consisting of rain gauge time series, high resolution vertically pointing radar (VPR) time series, and high resolution scanning radar images. Note that if $F_L(\vec{r}) = 0$ as occurs for rainfall, the $F_l(\vec{r})$ are also necessarily zero and thus $a_{l;L} = 0/0$ is indeterminate and so is discarded.

Correspondence to: G. L. Austin

1.1 Background and motivation

Recent work on the multiscaling characterization of rainfall (Harris et al., 1996; Menabde et al., 1997a, 1997b) has shown that rainfall can generally belong to one of two broad classes of statistics. One class is where the rain field is purely self-similar and can be modeled by self-similar multiplicative cascades. These are commonly referred to as multiscaling in reference to the scaling of moments (Appendix A). The other type is not multiscaling on its own, but by applying a transformation, such as taking absolute gradients or power-law filtering, it can be made multiscaling and is often referred to as multiaffine (Menabde et al., 1997a, 1997b; Vainshtein et al., 1994).

Both multiscaling and multiaffine fields have scaling Fourier power spectra of the form

$$P(k) \sim k^{-\beta}, \tag{3}$$

where β is the power law exponent usually determined by the slope of the spectrum on a log-log plot. Here, k is the frequency for a time series ($D = 1$) and wavenumber magnitude (i.e., $k = |\bar{k}|$) for a spatial image. For spatial data, $P(k)$ is found by averaging a D-dimensional Fourier power spectrum over all angles about $k = 0$ and is referred to as the isotropic spectrum of a D-dimensional field (Menabde et al., 1997a). β has some physical significance as a measure of smoothness (e.g., Davis et al., 1994).

Multiscaling and multiaffine fields can be easily distinguished by means of their spectral exponent, β. In theory multiscaling fields must have $\beta < D$ while multiaffine fields have $\beta > D$ (Menabde et al., 1997a, 1997b). In practice, however, a finite amount of data are used to estimate β and random uncertainties in the estimate of β may yield a value of β slightly larger than D even though the field is still multiscaling (Harris et al., 1997). From analyzing large amounts of rainfall data in the form of high time resolution rain gauge time series, vertically pointing radar (VPR) time series, and scanning radar images (PPI's), it is found that multiscaling fields are the exception rather than the norm in the scaling range of ~5 sec to several hours (or 100 m to 10 km for spatial data) (Harris et al., 1996; Georgakakos et al., 1994; Duncan, 1993). Therefore analysis of multiaffine fields is of paramount importance. In practice only rainfall processes accompanied by marginally unstable atmospheric stability are expected to have $\beta < D$ (Harris et al., presented at the 7th international conference on precipitation, Hawaii, 1998)

As already mentioned, a multiaffine field can be transformed into a multiscaling field by applying a transformation such as absolute gradients or power-law filtering (Lavallée et al., 1993) so that moment scaling analysis may be performed. These transformations, however, also present problems. Taking absolute gradients involves a loss of information and thereby increases the effects of noise on analysis results and procedures based on the scaling of moments such as estimating the $K(q)$ function (e.g., Davis et al., 1994; Harris et al., 1997) describes the effects of noise on $K(q)$ estimation). Power-law filtering also produces negative values and therefore absolute values or the choice of an arbitrary zero-level (DC offset) is used to make the field non-negative.

The work that follows is a continuation of the work started in Menabde et al. (1997a) where BDCs are first used as a method to analyze rainfall. The motivation for continuing this work lies in a number reasons. First and foremost, the adverse effect of unwanted noise if one is taking gradients, as mentioned above, (detailed in Harris et al. (1997)) prompted an investigation into applying BDC analysis directly to multiaffine fields (without taking gradients or power-law filtering). This is the most significant difference from the approach taken in Menabde et al. (1997a). Second, it is felt that greater attention can be given to the problems of parameter estimation for the purposes of modeling fields with a wider range of multiplicative cascades (only one cascade generator was considered in Menabde et al. (1997a)). Before these two goals are addressed, however, the details of BDC analysis need to be further investigated, particularly in light of the findings in Pedrizzetti et al. (1996). Addressing the details of BDC analysis thus forms a third goal in addition to the two primary motivations for this work, and also prompted some interesting theoretical points which are confined to the appendices. In particular, the theoretical link between the multiscaling formalism and the BDC formalism is addressed.

While the emphasis in this paper is on further developing BDC analysis as a tool, a long term goal of the authors is to gain an understanding of the link between scaling properties and meteorological descriptions of rain processes. Therefore, where scaling properties and parameters or rain data are derived, the general meteorological processes at hand are also mentioned.

1.2 Overview

The nature of the three goals just stated are such that they must be presented in a reverse order to that listed above. The paper begins with Sect. 2 where a brief overview of the theory of BDCs largely as presented in an earlier work by the authors (Menabde et al., 1997a) is included here for completeness and in order to clarify the notation and terminology used here. The theoretical link between BDC analysis and the multiscaling formalism, noted above, is mentioned in Sect. 2 and detailed in Appendix A. It should be mentioned that the theory of Sect. 2 and Appendix A holds only for multiscaling fields and is not applicable to multiaffine fields.

Sect. 3 focuses on details concerning the analysis and interpretation of results from BDC analyses. These are practical issues relevant to the parameter estimation methods in Sect. 4. Prompted by the results of Pedrizzetti

et al. (1996), this section continues the work presented in Menabde et al. (1997a) by investigating the BDC analysis method in greater detail. Illustrations of the method are provided by analyzing data in the form of high resolution rain gauge time series, 2D rainfall radar images, and multiplicative cascade models. From analyses of the latter, an important result is addressed in Sect. 3.4, and explained in greater detail in Appendix B, showing that bare canonical cascades are not scale similar, having important practical consequences for parameter estimation.

A general parameter estimation technique employing Monte Carlo techniques is introduced in Sect. 4. Whereas Menabde et al. (1997a) considered a specific model to characterize BDC analysis results, this paper considers a wider range of parameter estimates applicable to any model one chooses to use. The method is first illustrated using multiscaling fields and then applied to multiaffine fields by simply applying the same method for multiscaling fields on each individual scale.

2 Brief theory of breakdown coefficients

The theory of BDCs is elegant in that the only assumption is self-similarity from which all the other results follow. The formalism also deals with continuous fields, however in practice one usually applies it to discretized data such as a digitized radar image or time series. The following contains the definitions used, the precise assumptions of self-similarity made, and a brief account of the theory that follows as developed largely by Novikov (1990, 1994 and references within).

2.1 Definitions

From the definition of a BDC, (2), given any intermediate length, ρ, where $l < \rho < L$ and $V_l \subset V_\rho \subset V_L$,

$$a_{l;L} = a_{l;\rho}\, a_{\rho;L}. \tag{4}$$

The principle and only assumption made here is that $a_{l;L}$ are random variables which depend only on the scale ratio l/L which allows one to write the q^{th} moments of (2) as

$$\left\langle a_{l;L}^q \right\rangle = \left\langle a_{l;\rho}^q \right\rangle \left\langle a_{\rho;L}^q \right\rangle. \tag{5}$$

This relation is referred to here and below as the scale similarity of moments and is often assumed. While theory suggests that this is a sufficient and necessary condition for scale similarity, it has been shown that turbulence velocity data do not exactly satisfy Eq. (5) (Pedrizzetti et al., 1996) and is examined further below for the case of rainfall.

Since $a_{l;L}$ and its moments depend only on the scale ratio, l/L, the general solution of (5) is

$$\left\langle a_{l;L}^q \right\rangle \sim (l/L)^{-\mu(q)}. \tag{6}$$

In turbulence, one has the additional condition that $\mu(0) = 0$. For rainfall, however, the condition, $\mu(0) = 0$, is not exact since the presence of regions or periods of zeroes (dry areas or periods) in the data cause $\mu(0) \neq 0$. Relation (6) brings to light the important point that BDC analysis is not a method entirely different to the multiscaling picture but rather a complimentary alternative with theoretical links to the multiscaling formalism further developed in Appendix A.

2.2 Infinitely divisible distributions of breakdown coefficients

The random variables, $a_{l;L}$, are by definition restricted in range $0 \le a_{l;L} \le (L/l)^D$ (i.e., $F_l l^D \le F_L L^D$ by mass conservation) and it is thus convenient to define a new random variable

$$x_{l;L} = -\ln\left(\frac{F_l l^D}{F_L L^D}\right) = -\ln\left(a_{l;L}\left(\frac{l}{L}\right)^D\right), \tag{7}$$

where $0 \le x_{l;L} < \infty$ and is loosely referred to here as the log-BDC. The property (4) for multiscaling fields may now be written

$$x_{l;L} = x_{l;\rho} + x_{\rho;L}. \tag{8}$$

If the field is subdivided so as to introduce n intermediate scales of size ρ_i, between l and L so that $l/\rho_1 = \rho_1/\rho_2 = \ldots = \rho_n/L = (l/L)^{1/n}$ and $V_l \subset V_{\rho_1} \subset V_{\rho_2} \subset \ldots \subset V_L$ one has

$$x_{l;L} = x_{l;\rho_1} + x_{\rho_1;\rho_2} + \ldots + x_{\rho_n;L}. \tag{9}$$

The variables in the sum are independently and identically distributed variables whose distribution is dependent only on the scale ratio, $(l/L)^{1/n}$, and so dropping the subscripts one writes for their probability density

$$p(x, (l/L)^{1/n}) = p(x, \rho_i/\rho_{i+1}). \tag{10}$$

Therefore $p(x, (l/L)^{1/n})$, which is the pdf of the log-BDCs, belongs to the class of infinitely divisible distributions as found in Feller (1966, Chap. VI.3) where (9) and (10) alternatively define $p(x, l/L)$ as equal to the n-fold convolution of $p(x, (l/L)^{1/n})$ with itself.

3 Breakdown coefficient analysis

The pdf of the logarithm of the BDC, $p(x, l/L)$, is the focus of the analysis in this paper and its properties and method of computation are reviewed in this section. While the theory in the previous section is relatively straightforward it poses some questions as to the details of how BDC analysis is performed. A number of these issues are raised in detail in Pedrizzetti et al. (1996) (hereafter referred to as PNP) and in much greater detail than here. Most of the tests and verifications performed in PNP were repeated using rainfall

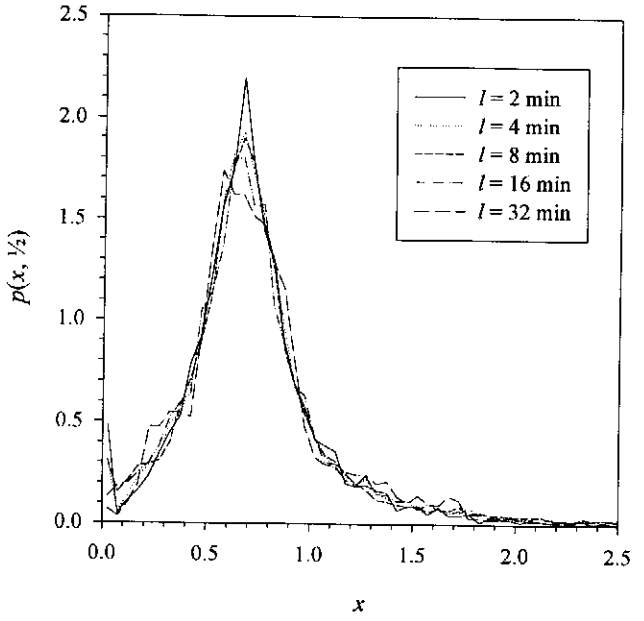

Fig. 1. Breakdown coefficient densities for a rain gauge time series showing the visual degree of scale similarity. The time series was collected at 15 second resolution for 34 hours. Data are collected at Arthur's Pass, New Zealand, November 5-7, 1994.

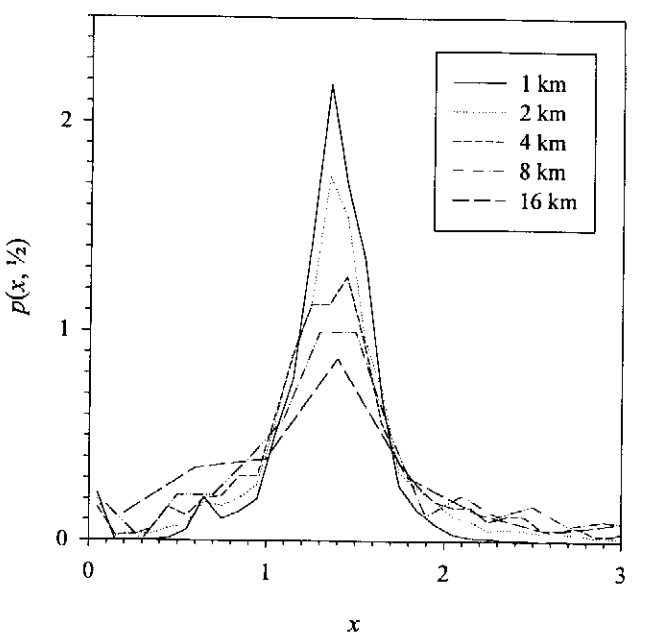

Fig. 2. $p(x)$ densities for a multiaffine spatial rain field. BDCs for 2D images from a large C-band radar (100 km range and 1 km resolution) from which the BDCs at scales 1 km to 6 km were computed. The histogram features bin widths of 0.1 and was computed from 5 images per radar over the period of an hour.

data with similar results and so are not reported here in great detail. The issue of the relative locations of the regions used to calculate each BDC is described below as it has an important bearing on the analysis method. The effect of relative locations of the regions leads to what is called the Δ factor, which is important when empirically verifying Eq. (5). Δ is also used at the end of this section to relate $\mu(q)$ in (6) to the moment scaling function, $K(q)$, used elsewhere in the literature (e.g., Davis et al., 1994; Lavallée et al., 1993; Schertzer and Lovejoy, 1987).

3.1 General concept of scale similarity and breakdown coefficients

Using a rainfall time series as a sample data set, the densities $p(x, l/L = ½)$ (written $p(x, ½)$) are shown in Fig. 1 for a number of scales. In general, scale similarity is implied when the pdf of the BDCs or log-BDCs is independent of scale as is the case for Fig. 1. The data used in Fig. 1 have a Fourier spectral exponent, $\beta = 0.94 \pm 0.04$ and so $\beta < D = 1$ which agrees with the scale similarity observed. This data set has been analyzed elsewhere in the literature (Harris et al., 1996), representing a stable rainfall process in a high altitude alpine region, where the stability of the atmosphere is partially a result of the orographic flow over mountains (Purdy et al., prepared for Meteorological Applications, 1998).

By contrast, Fig. 2 shows $p(x, ½)$ for different scales computed from spatial rainfall data which are clearly not scale similar since the $p(x, ½)$ are clearly dependent on scale. The data used to compute $p(x, ½)$ at each scale in Fig. 2 consist of a rain field derived from a New Zealand Met Service C-band radar having 1 km resolution. The field has a scaling isotropic power spectrum with $\beta = 2.31 \pm 0.02$ and is thus an example of a multiaffine field. This rain field is part of a large scale warm frontal rain band.

The decrease in the width of $p(x, l/L)$ with scale is characteristic of multiaffine rainfall fields and reflects the self-affine nature of rainfall. In other words the fluctuations decrease in amplitude with scale and so $a_{l;L}$ approaches one as scale decreases indefinitely (see Marshak et al., (1994, Fig. 2) for a nice illustration of this effect in bounded cascades).

3.2 BDC computation: Relative displacements and the Δ factor

From existing literature on scale-similarity and BDCs (Pedrizzetti et al., 1996; Kida, 1991) it is evident that there are a number of ways to compute BDCs. The main issue discussed in this section, and to which PNP is largely devoted, concerns the fact that in (2) one has to address how the positions of the local densities are chosen. In other words one is concerned with the relative locations of $\vec{r}$ and $\vec{r}^{\,*}$.

As in PNP one may include the explicit dependence on the relative displacement of the two segments in (2) and (7) by writing the variables $a_{l;L}$ and $x_{l;L}$ as $a_{l;L}(\Delta)$ and $x_{l;L}(\Delta)$, respectively, where

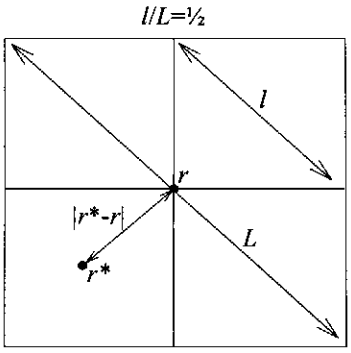

Fig. 3. Schematic of principle quantities used in the computation of BDCs in a 2D data set as referred to in the text.

$$\Delta = \frac{|\vec{r}^{\,*} - \vec{r}|}{L - l}. \qquad (11)$$

For example, in a time series, Δ = ½ corresponds to BDCs computed by taking the ratios of the rightmost and leftmost element of size l fully contained within the region of size L. In 2D and 3D digitized images, the scales L and l are chosen here to correspond to the length of the diagonals of pixels of the differing sizes (Fig. 3). With these definitions of scale, if $\Delta > ½$ then the regions are not chosen according to an inclusive rule in which the volumes are included within each other (i.e., $V_l \subset V_L$) but rather a non-inclusive rule such as that referred to in Kida (1991) where $|\vec{r} - \vec{r}^{\,*}| \le (L-l)$ and thus $\Delta \le 1$. In this paper Δ is restricted to $\Delta \le ½$ for reasons made clear below and in Appendix A.

Scale similarity is observed for any fixed value of Δ, yet the effect of different Δ is illustrated in Fig. 4 for rainfall data from weather radar imagery, where it is evident that the width of $p(x, l/L, \Delta)$ increases with increasing Δ. This is true for breakdowns of all scale ratios. This dependence on Δ is observed for BDCs from all cascade simulations as well as measured data and is a consequence of correlations between data points as stated in PNP.

As indicated in PNP, the observed dependencies and differences in BDC distributions on Δ suggests that Δ should be kept fixed in the breakdown process. Limited data sets also require optimal use of the data and for fixed Δ, only breakdown ratios of l/L = ½ result in all the available data being used at each scale. Therefore in this work breakdowns of l/L = ½ , and Δ = ½ will be used exclusively so that the explicit dependence of $p(x)$ on Δ and l/L is dropped below. Thus the reasons for using Δ = ½ are that: 1) Δ = ½ results in optimal use of the data, 2) the breakdown process is conceptually the reverse of a cascade process, and 3) Δ = ½ is the value for which (6) is the same as the moment scaling relation used elsewhere in the literature (see Appendix A).

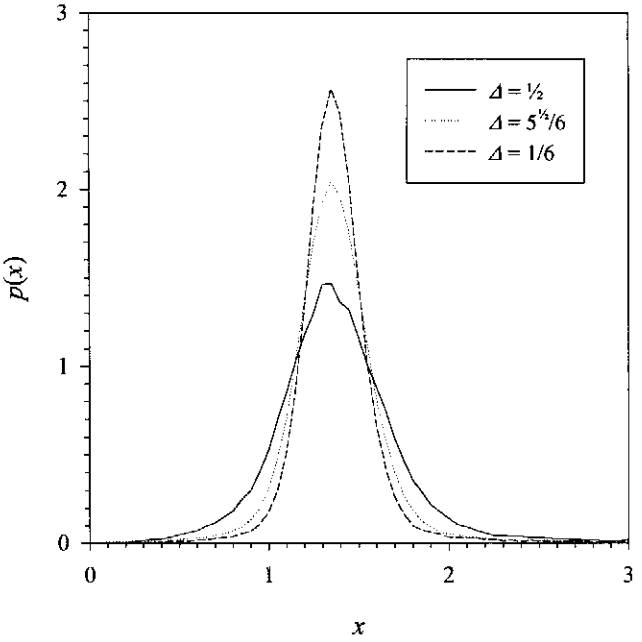

Fig. 4. Dependence of $p(x)$ on Δ. The $p(x)$ were computed from an ensemble of two high resolution radar images 4 minutes apart. Breakdown was from pixels of size l = 200 m over size L = 800 m (i.e., l/L = ¼). The data consisted of rain rates (R) computed from the reflectivity (Z) using $Z = 200R^{1.6}$. The various values of Δ correspond to taking either the four corner pixels, the eight non-corner outer pixels or the four inner pixels for Δ = ½, 5½/6 or 1/6, respectively.

3.4 Relation between cascade generators and $p(x)$

Before parameter estimation is addressed, some understanding of the relation between $p(x)$ and cascade generators is necessary as this will determine whether parameter estimates are relevant to any subsequent cascade modeling of rainfall.

Multiplicative cascade simulations are used to generate large statistical samples with known properties which can then be used to illustrate the features of BDC analysis. A wide variety of cascades are in current use and so it is necessary to briefly clarify the types of cascades used in this study.

The simulations used here are discrete random cascades (e.g., Gupta and Waymire, 1993) with a branching number, b = 2 for time series and b = 4 for 2D spatial data (i.e., $b = 2^D$). Models are either microcanonical or canonical in construction. Microcanonical cascades are those in which the 2^D weights, W, have a mean of exactly one (i.e., $\langle W_i \rangle = 1$) at each step in the cascade, while for canonical cascades the expectation of the weights is unity. The microcanonical models used below are formed by generating b independent numbers, y_i, and normalizing them so as to obtain the multiplicative weights,

$$W_i = \frac{y_i}{\frac{1}{b}\sum_{j=1}^{b} y_j}. \qquad (12)$$

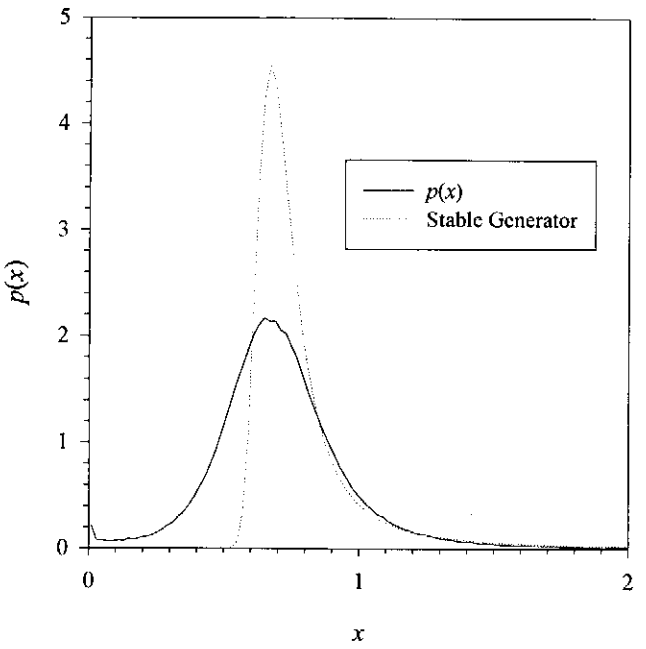

Fig. 5. Comparison of $p(x)$ estimated for 100 16384 point canonical log-stable cascades and the generator used to create the cascades. The generator used was a stable distribution with $\alpha = 1.1$ and $\sigma = 0.07$.

The variables, y_i, are referred to here as the pre-normalized weights.

There are many different methods used to generate the weights (e.g., Gupta and Waymire, 1993). Models with two parameters allow an extra degree of freedom when fitting, and therefore here the weights, W (for canonical cascades), or pre-normalized weights, y (for microcanonical cascades), are drawn from either a log-stable or log-gamma distribution. In other words $W_i = e^{\Gamma}$ or $y_i = e^{\Gamma}$ where the generator, Γ, is either extremely asymmetrically stable distributed ($\Gamma \sim S_\alpha(\sigma, \beta = 1)$) or gamma distributed ($\Gamma \sim g(\nu, \sigma)$). The stable random variables are generated using the RSTAB routine found in Samorodnitsky and Taqqu (1994). Gamma variables are generated using routines based on the rejection method as outlined in Devroye (1986, p. 410-415).

Canonical cascade simulations

Canonical cascades are often used to simulate rainfall and other geophysical fields (e.g., see Schertzer and Lovejoy (1987) and Gupta and Waymire (1993)) owing to their simplicity and ease of use. Canonical cascades may be iterated to a final scale ratio (bare cascades) or iterated beyond a final scale ratio and then averaged back up to the final scale ratio (dressed cascades). When analyzing the scale-similarity of canonical cascades one finds that bare cascades show poor scale similarity over the smallest scales. This can be explained by considering the construction and breakdown of a canonical cascade (see Appendix B).

From Appendix B it is also apparent that $p(x)$ will not be the same as the density of the generator, Γ. This means that a canonical log-stable cascade with parameters σ and α for the generator will not yield a $p(x)$ which is stable with the same parameters σ and α. This is not only due to the dressing factors but also due to the fact that the denominator (in (B4) for example) is equal to unity only on the average and not on each step. Thus one expects a broader log-BDC distribution, $p(x)$, than that of the generator. In other words the breakdown process is microcanonical in the sense that there is conservation on every step unlike canonical cascades and the breakdown thus disagrees with the construction of the field as illustrated in Fig. 5. While the apparent difference for this specific example seems extreme, the generator density shown in Fig. 5 was estimated by a canonical cascade model fit to BDC data from the same time series used in Fig. 1. In general one observes that the difference between $p(x)$ and the generator as shown in Fig. 5, decreases with increasing σ and α.

Microcanonical cascade simulations

Microcanonical cascades are different from canonical cascades with regards to BDC analysis because by construction $\langle W_i \rangle = 1$ exactly at each step in the cascade so that the denominator in (B4) is unity. This means that $p(x)$ is identically distributed to $p(\ln(W(L/l)^D)$ or in other words $p(x) \sim p(\ln(W))$ to within a translational shift $D\ln(L/l)$ and $x \sim \ln(W)$. The problem with microcanonical cascades, however, is that given a specific generator for y_i, there is no simple analytical form for the multiplicative weights, W_i. Conversely, an estimation of how W_i is distributed for a data set says little about the generator, y_i, needed to simulate data with the same characteristics. This is an important factor considered in Sect. 4.

4 Parameter estimation using a Monte Carlo technique

An estimated log-BDC density, $p(x)$, may be parameterized by a least-squares fitting procedure. For scale similar data, infinitely divisible distribution densities may be fitted, and two popular examples are the gamma distribution and the stable distribution. The gamma distribution has an analytical form while the stable distribution does not and so in the case of the latter a Monte Carlo approach is taken by generating histograms from a large number of stable generated numbers and fitting this histogram to $p(x)$ for the data.

While estimation of infinitely divisible distribution parameters is a useful method of characterizing the intermittency of the data, the discussion above in Sect. 3.4 indicates how the parameters may not be useful for cascade modeling purposes. In order to estimate cascade model

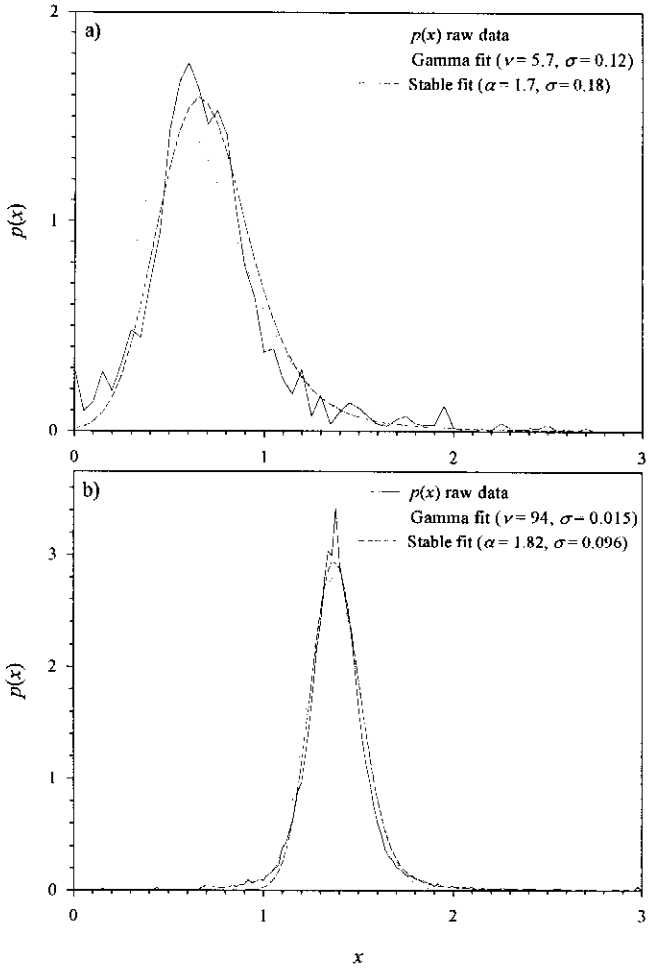

Fig. 6. Curve fits for estimated $p(x)$ derived from a) a 8192 point time series at 15 second resolution and b) an ensemble of five 64×64 200m resolution spatial radar rainfall images with each image two minutes apart. In each case the $p(x)$ curve is shown (solid line) together with a best fit of a gamma distribution (dotted line) and stable distribution (dashed line). For the time series data $\chi^2 = 25$ for the gamma fit and $\chi^2 = 14.1$ for the stable fit giving χ^2 exceedence probabilities of 17% and 80%, respectively. For the spatial data $\chi^2 = 390$ for the gamma fit and $\chi^2 = 278$ for the stable fit giving χ^2 exceedence probabilities near zero.

parameters, a Monte Carlo method must also be used, this time generating, for example, histograms of renormalized weights for the microcanonical case. This is discussed in greater detail below.

For the case of parameter estimation of multiaffine fields, the fitting procedure used is the same as for multiscaling fields with the key difference being that a fit is performed for $p(x)$ at each scale, since $p(x)$ is not scale similar.

4.1 Parameter estimation of multiscaling fields

Infinitely divisible distribution parameter estimates

As shown above, the pdfs of the logarithm of BDCs belong to the class of infinitely divisible distributions including stable (of which the Gaussian is a special case) and gamma

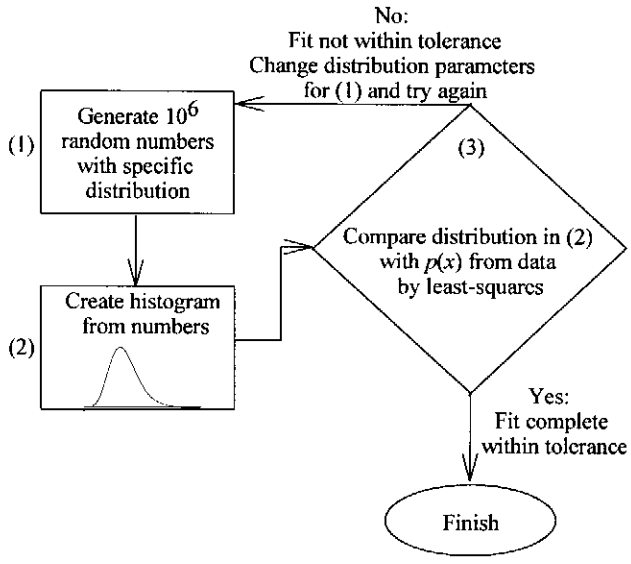

Fig. 7. Schematic diagram of Monte Carlo fitting procedure. Step (1) either generates a) numbers from an appropriate generator, b) renormalized numbers from an appropriate generator (microcanonical model) or, c) BDCs from a canonical cascade created from an appropriate model. On failure of step (3), which represents the minimization routine, slightly different parameters are chosen for the generator in step (1).

distributions, to name a few. Of this class of distributions there is no physically based reason to choose any one distribution over an other. Choice is made simply on the ability of a theoretical distribution's fit to the observed $p(x)$. The fact that x is positively defined with long tails out to large positive x is also a consideration in choosing asymmetric distributions. Also, when fitting model densities to $p(x)$ it is simply convenient to have a sufficient number of free parameters. The gamma density has two free parameters: a scale parameter, σ, and a shape parameter, ν. In multiscaling and multifractals, the stable density, $S_\alpha(\sigma, \beta, \mu)$, is restricted to the extremely asymmetric case with $\beta = 1$ so that the moments of the log-stable distribution are finite (Samorodnitsky and Taqqu, 1994, p. 52 and references within). In this case, the stable distribution also has two free parameters with α being the shape parameter and σ is the scale parameter. The translational shift parameter, μ_S (i.e., $S_\alpha(\mu_S) = S_\alpha(0) + \mu_S$ where the subscript, S for 'stable', is included to avoid confusion with the exponent $\mu(q, \Delta)$ in (6)), is fixed to $\mu_S = \log(L/l)$, in the fitting procedure.

The simplest procedure involves fitting a known distribution in closed form, such as the gamma distribution, to the experimental $p(x)$. Examples of fitting gamma distributions to $p(x)$ for rain gauge time series and spatial radar data are shown in Fig. 6.

The temporal data is an example of data with embedded convection having moderately high intermittency. The spatial data was an example of rain associated with a cold front and features low intermittency. The intermittency of the field is reflected by σ. A high σ value indicates high intermittency.

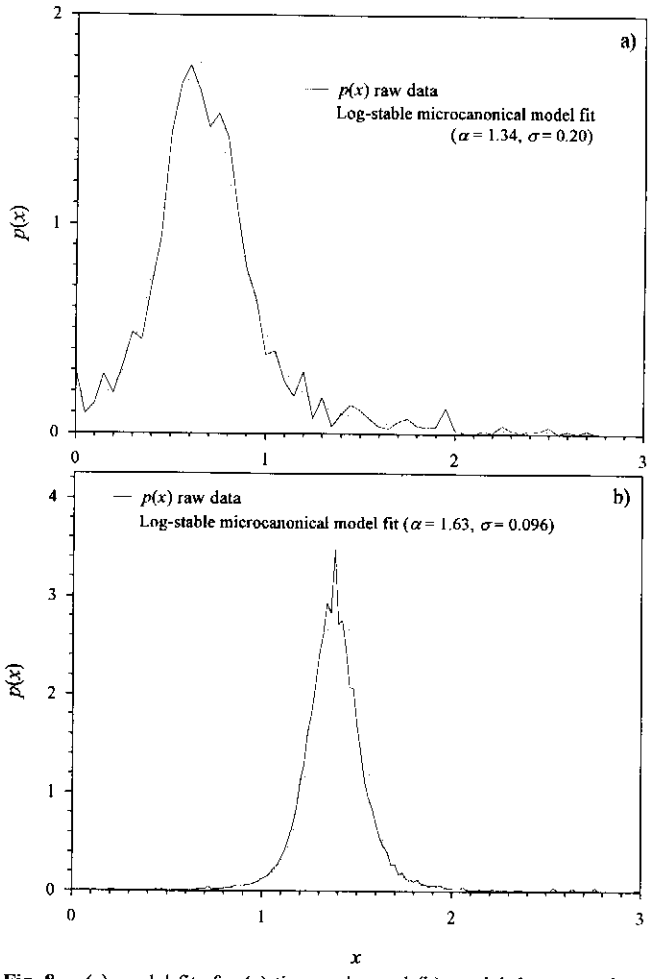

Fig. 8. $p(x)$ model fits for (a) time series and (b) spatial data assuming a log-stable microcanonical model. The data used is identical to that used in Fig. 7. Compared with Fig. 7 the fits are better with χ^2 values of 1.8 and 140 for the time series and spatial data, respectively. This results in χ^2 exceedence probabilities of near 1 and 0, respectively.

Also shown in Fig. 6 for comparison are the stable distribution fits and here the data are fitted using a Monte Carlo method. Generation of distributions from, say, 10^6 numbers drawn from a random stable number generator such as RSTAB (Samorodnitsky and Taqqu, 1994) can be fitted by minimizing χ^2 or the least squares difference between the generated stable distribution and the empirical $p(x)$ based on the data. For this paper this was accomplished using the routine AMOEBA.C (Press et al., 1992).

Cascade model parameter estimates

As shown in Sect. 3.3 and Fig. 6, the distribution of the log-BDCs are not equal to the distribution of the generator used to create the field. Therefore Monte Carlo methods (shown schematically in Fig. 7) must be used to estimate the parameters for the generator that produces the desired log-BDC distribution. In the case of canonical models, the

Table 1. Model scale parameter, σ, and standard deviation of distributions of log-BDCs.

Scale	Model σ	Standard Deviation
1 km	0.17	0.32
2 km	0.25	0.42
4 km	0.35	0.59
8 km	0.50	0.70
16 km	-	0.98

cascade must be constructed and then used to estimate the log-BDC distribution. Here there is a computational advantage for estimating microcanonical cascade parameters. Since the log-BDC distribution for a microcanonical cascade is equal to the distribution of the log of the weights, distributions are generated by drawing weights normalized as in (12) and again these distributions may be fitted to the $p(x)$ curve by minimizing least squares. The weights are produced in quantities of 2^D with the y_i's being drawn from a convenient distribution. Again either the log-gamma or log-stable distributions are used to generate the y_i's as they allow for two parameters. Fits and parameter estimates for a log-stable microcanonical model are shown in Fig. 8, using the same data as that used in Fig. 6.

If one is to use this Monte Carlo method to estimate parameters for a canonical model it is necessary to draw the fitting distributions by creating appropriately dressed cascades (see Appendix B) for step (1) in Fig. 7. This is very time consuming for two simple reasons: First, the cascades must be dressed which in practice is at least an extra six or seven steps in the cascade, and second, the act of first creating a cascade and then breaking it down to find its BDCs adds yet more time to the procedure.

4.2 Parameter estimation of multiaffine fields

As already mentioned, multiaffine fields are the norm in rain fields rather than the exception, and so in general $p(x)$ densities are a function of scale as in Fig. 2. It is convenient to include the explicit dependence on scale and write $p(x)$ as $p_l(x)$. The methods of $p(x)$ parameterization in Sect. 4.1 are still applicable but different distribution parameters are found for each scale.

The recent interest in bounded cascade models (Marshak et al., 1994; Menabde et al., 1997b and references therein) which feature a scale dependent generator suggests verifying whether the measured change in $p_l(x)$ for rain fields is in accordance with that assumed for bounded cascade models. There are many different bounded cascades in the literature, but the one with the most conceptual link to the type of $p_l(x)$ behavior shown, for example by Fig. 2, is the log-stable bounded cascade (Menabde, submitted to Nonlinear Processes in Geophysics, 1997) with multiplicative weights, $W_n = e^{\Gamma_n}$, determined by the generator

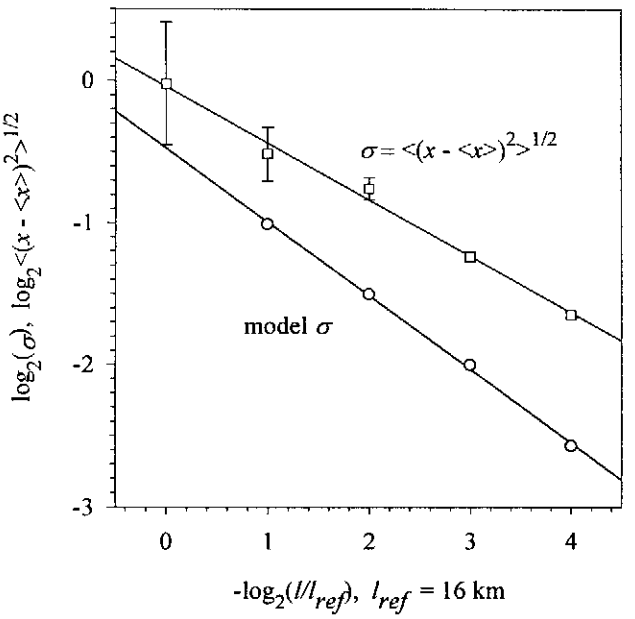

Fig. 9. Standard deviations of BDC distributions and model scale parameter as a function of scale for a multiaffine data set. The upper plot (squares) represents the standard deviation for each $p(x)$ in Fig. 2 from l = 1 km upwards. The lower plot (circles) represent the model scale parameter, σ, estimated by fitting microcanonical stable log-BDCs to each $p(x)$ in Fig. 2. The slope of the upper line (squares) is 0.42 ± 0.03 while the other is 0.48 ± 0.01 and is equal to H. The model σ at 16 km could not be estimated reliably due to insufficient data.

$$\Gamma_n = S_\alpha(\sigma_n), \tag{13}$$

$$\sigma_n = \sigma_0 2^{-nH}, \; H > 0, \; n = 0, 1, 2\ldots, \tag{14}$$

where n is the step of the cascade. In other words the generator is stable with a scale parameter, σ_n, which is step dependent. In fact σ_n is scaling since $n \sim \log_2(1/l)$. The parameter, σ_0, is simply the scale parameter of the generator at the largest scale in the cascade when n = 0. The cascade is bounded in the sense that as $n \to \infty$, one has $\sigma_n \to 0$ and $\langle W_n \rangle \to 1$.

The notion of a scaling scale parameter in the generator was first verified here by simply finding the standard deviation, σ_p, for $p_l(x)$ at each scale and verifying whether σ_p scales. Using the data from Fig. 2 (explained in Sect. 3.1), for scales of l = 1 km to 16 km, the standard deviation was estimated from each $p_l(x)$ using

$$\sigma_p^2 = \langle x^2 \rangle - \langle x \rangle^2 = \frac{\sum x^2 p_l(x)}{\sum p_l(x)} - \left(\frac{\sum x p_l(x)}{\sum p_l(x)} \right)^2. \tag{15}$$

The scaling behavior of σ_p is shown by a linear relation on a plot of $\log_2(\sigma_p)$ vs $-\log_2(l/l_{\text{ref}})$ where l_{ref} is a reference scale set to be the largest scale. The result is shown in Table 1 and the top plot (squares) of Fig. 9 for l_{ref} = 16 km. Error bars for the upper plot represent the standard error in the standard deviation estimated in the usual way by $((\mu_4 - \sigma_p^2)/(4N\sigma_p^2))^{1/2}$ (e.g., Spiegel, 1972, p. 144), where N is the number of points contributing to each distribution, $p_l(x)$. The seemingly unusual choice for the abscissa is made in order to remain consistent with the conceptual model of the bounded cascade in (13) and (14) so that the standard deviation may be expressed as $\sigma_p = 2^{-nH}$. H characterizes the rate at which the standard deviation of the densities decreases with scale and obtained simply by the slope, $H = 0.42 \pm 0.03$.

The bounded cascade model (13) and (14) is canonical, yet the effect on scale similarity that dressing imposes makes it impractical for fitting. Thus the model used here to reproduce multiaffine fields is a microcanonical model in which the pre-normalized weights $y_n = e^{\Gamma_n}$ are as described by (13) and (14). The scale parameter of the generator changes with step while the shape parameter, α, is assumed to remain fixed. α is estimated at the first step of the breakdown process (i.e., l = 1 km) and kept fixed for the fitting of the remaining $p_l(x)$. In practice α fluctuates a bit which affects model estimates of σ_n. A one parameter fit using AMOEBA.C as in Sect. 4.1 is used to obtain the scale parameter, σ_n, at each length scale. The results are tabulated in Table 1 and shown by the bottom plot (circles) in Fig. 9. The model scale parameter, σ, could not be estimated reliably at 16 km since at this resolution there is insufficient data (64 points) to fit a model density. For scales of 1 km to 8 km the relation was linear and the estimate for the slope was equal to $H = 0.48 \pm 0.01$.

5 Summary and conclusion

Breakdown coefficient (BDC) analysis has been developed in the turbulence literature by Novikov (1990, 1994, and references therein) and applied to rainfall by the authors here and initially in Menabde et al. (1997a). The density of the log-BDCs, $p(x)$, is proven to be an analysis method sensitive to scale similarity as shown in Pedrezzetti et al. (1996). This work promotes BDC analysis as a method complimentary to the multiscaling approach, used extensively in the geophysical sciences, with well defined theoretical links. In addition to sensitivity, the method has the advantage of being conceptually accessible, particularly in its ability to help visualize differences between multiaffine and multiscaling fields while using the same method to study both types of field.

This work is a continuation of the previous paper on applying BDC analysis methods to rainfall (Menabde et al., 1997a) by incorporating some of the findings in Pedrizzetti et al. (1996). In particular, the issue is raised of relative displacements in the breakdown volumes. This is represented by the factor, Δ. Some arguments are presented for using Δ = ½. First that Δ = ½ results in the optimal use of data. Second, from a theoretical standpoint, Δ = ½ is empirically found to be the value for which the BDC moment scaling exponent, $\mu(q, \Delta)$, is equivalent to $K(q)$ (Appendix A).

Technical details aside, the main thrust of this paper is the development of a general parameter method applicable to both multiscaling and multiaffine fields. While fitting various distributions to $p(x)$ characterizes the field, things are complicated somewhat when one wants to estimate parameters useful for cascade modeling fields with the same statistics. Bare canonical cascades are not scale similar and need to be at least partially dressed to show a sufficient degree of scale similarity as shown in Appendix B. Perhaps a more significant result is that even for a scale similar (i.e., dressed) canonical cascade, one cannot easily retrieve the cascade generator in the sense that the $p(x)$ density computed for the cascade bares no simple relation to the distribution density of the generator. This makes microcanonical cascades attractive since the log-BDC variable, x, is equal to the log of the multiplicative weights used to produce the cascade.

The notion of retrievable weights for microcanonical cascades has an important consequence for cascade model parameter estimates. Given a data set with associated density, $p(x)$, the parameters for a microcanonical cascade model that is capable of producing more data with similar $p(x)$ involves creating a histogram of multiplicative weights which matches the observed $p(x)$ for the original data. The histogram is created using a Monte Carlo method where a large number of weights are generated using specific parameters and the parameters are tweaked to fit the observed $p(x)$. On the other hand canonical cascade model parameters can only be estimated by a more computationally intensive Monte Carlo method where entire random cascades are constructed and then broken down to compute BDCs from which synthetic $p(x)$ densities are fitted to the original $p(x)$.

Multiaffine data are characterized by log-BDC densities, $p(x)$, which are scale dependent and broaden with increasing scale. More interestingly, they broaden in a scaling fashion. That is, empirical observation show that the variance of the log-BDCs increase in a power-law fashion. Parameterizing the $p(x)$ at each scale according to various microcanonical cascade models also result in generator scale parameters, that increase in a power law fashion with scale. This corresponds well with the concept of bounded cascades proposed by these and other authors (e.g., Marshak et al., 1994; Menabde et. al., 1997b).

Having addressed, to a certain extent, the technical and methodology issues of BDC analysis, more focus is now needed on relating parameter estimates to meteorological processes. As study is currently underway whereby the emphasis is put on meteorological classifications of rainfall processes and their associated scaling properties.

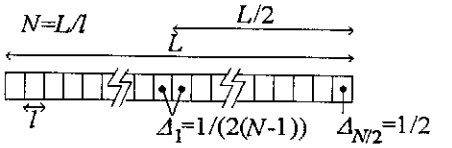

Fig. A1. Schematic diagram showing Δ factor for breakdown of discrete field with $N = 2^n$ points. In general there are $N/2$ different Δ's equaling $\Delta_k = (2k\text{-}1)/(2(N\text{-}1))$ for $k = 1, 2, \ldots, N/2$.

Appendix A. BDC analysis and moment scaling

The definition of a multiscaling field is one for which

$$< R_l^q > \sim (l/L)^{-K(q)}, \tag{A1}$$

where R_l represents the field at resolution l and the scale L is usually taken to be the largest scale of the field. $K(q)$ is the moment scaling function already referred to above.

Given the similarity between Eq. (6) and Eq. (A1) it is interesting to show if there is a link between these two relations. First, it is important to rewrite relation (6) to include explicit dependence on Δ as discussed in Sect. 3.2 and as done in PNP so that

$$\left\langle a_{l;L}^q(\Delta) \right\rangle \sim (l/L)^{-\mu(q,\Delta)}. \tag{A2}$$

Consider the case where L remains fixed by choosing, say, L to be the maximum scale over which scaling is observed. In this case the dependence on L and R_L is dropped (or equivalently let $L = R_L = 1$) and (A2) may be rewritten as

$$\left\langle R_l^q(\Delta) \right\rangle \sim l^{-\mu(q,\Delta)}. \tag{A3}$$

Given the similar forms of (A1) and (A3) it is important to establish the relation between the often used exponent function $K(q)$ and the exponent, $\mu(q, \Delta)$.

For a discrete field of N_l points at resolution, l, only two points in the field have the same Δ so that the moment, $< R_l^q >$, in which BDCs with different Δ's are all mixed together may be represented by

$$\left\langle R_l^q \right\rangle = \frac{2}{N_l} \sum_{k=1}^{k=N_l/2} \left\langle R_l^q(\Delta_k) \right\rangle = \frac{2}{N_l} \sum_{k=1}^{k=N_l/2} l^{-\mu(q,\Delta_k)} \sim l^{-K(q)}. \tag{A4}$$

In practice the $K(q)$ function is often computed by computing the moments, $< R_l^q >$, at the highest resolution, l, and then degrading the resolution by averaging neighboring pixels to a field with half as many points and resolution, $2l$, and computing the moments again and so on. This requires a field with $N_l = 2^n$ points with n an integer. In this case Δ assumes the values,

$$\Delta_k = \frac{2k-1}{2(N_l-1)}, \quad k = 1,2,\ldots N_l/2. \tag{B5}$$

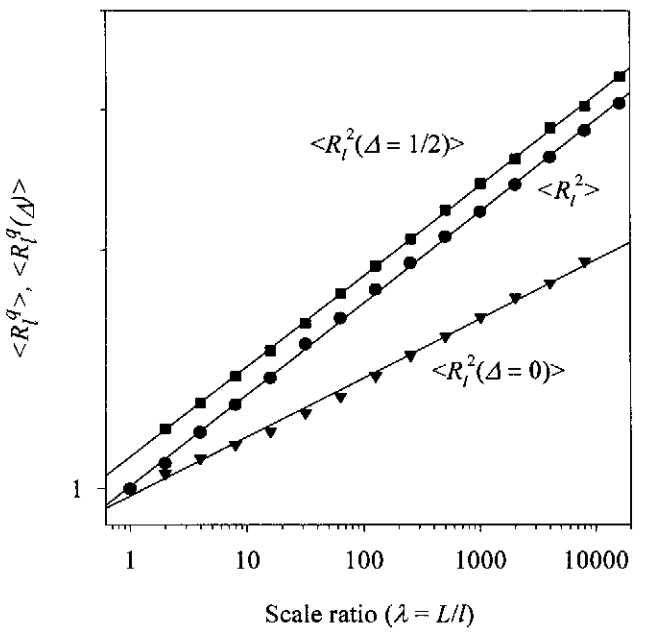

Fig. A2. Scaling moment analysis comparing the exponents $K(q)$ and $\mu(q,\Delta)$ for q=2. The exponents are given by the slope of each curve and were found to be $\mu(2, ½) = 0.115$, $K(2) = 0.113$, and $\mu(2, 0) = 0.074$, respectively. The data set analyzed to obtain these moments consisted of 2×10^4 16384 point microcanonical cascades for $<R_l^q(\Delta)>$ and 200 16384 point cascades for $<R_l^q>$.

Fig. A1 illustrates a schematic diagram depicting this procedure and the quantities in relation (A4) and (A5). As the process of coarsening increases, l increases, N_l decreases, and there are fewer Δ_k's.

For large enough N (i.e., large data sets at small scales) the sum in (A5) can be represented as a Riemann integral and applying the method of steepest descents one has,

$$\left\langle R_l^q \right\rangle \sim \int_0^{1/2} l^{-\mu(q,\Delta)} d\Delta \sim l^{-\mu(q,\Delta_*)} \sim l^{-K(q)}, \qquad \text{(A6)}$$

where Δ_* is given by the condition for which $\mu(q, \Delta)$ is maximum. In practice the maximum values of $\mu(q, \Delta)$ occur when $\Delta = ½$ and in Fig. A2 one may see that $K(q)$ is quite close to $\mu(q, \Delta = ½)$ for an example in which an ensemble of 10^4 microcanonical cascades was analyzed. The high number of cascades is necessary to get good statistics, keeping in mind that one cascade only yields two points to $< R_l^q(\Delta) >$ for each Δ at each scale, l.

Appendix B. BDCs of bare canonical cascades

Following the notation of Kahane and Peyriere (1976) used elsewhere in the literature (Gupta and Waymire, 1994; Harris et al., 1996), an n-step bare cascade may be written as

$$R_n(i_1, \ldots, i_n) = R_0 W(i_1) W(i_1,i_2) \ldots W(i_1, \ldots, i_n), \qquad \text{(B1)}$$

while a dressed cascade may be written as

$$\bar{R}(i_1,\ldots i_n) = R_n Z_{N-n}(i_1,\ldots i_n). \qquad \text{(B2)}$$

Z_{N-n} is the random uncorrelated dressing factor given by

$$Z_{N-n}(i_1,\ldots i_n) = 2^{n-N} \sum_{i_{n+1},\ldots,i_N} W(i_1,\ldots,i_{n+1}) W(i_1,\ldots,i_{n+2}) \ldots W(i_1,\ldots,i_N). \qquad \text{(B3)}$$

For purposes of illustration the example considers BDCs computed for $\Delta = l/L = ½$ but still holds for other scale ratios and Δ. Consider the BDCs of the bare process (B1) at the smallest scale. Because neighboring pixels have common parents in the cascade the parents factor out to give

$$a_{l;L} = \frac{W(i_1, \ldots, i_n)}{\frac{1}{2}(W(i_1, \ldots, i_n) + W'(i_1, \ldots, i_n))}, \qquad \text{(B4)}$$

where W and W' are neighbors at the smallest scale. At the next largest scale one scale of dressing has effectively occurred so that the BDCs are given by

$$a_{l;L} = \frac{W(i_1, \ldots, i_n) Z_1}{\frac{1}{2}(W(i_1, \ldots, i_{n-1}) Z_1 + W'(i_1, \ldots, i_{n-1}) Z_1')}, \qquad \text{(B5)}$$

where WZ and $W'Z'$ are neighbors. Because of the effective increasing degree of dressing at larger scales BDCs in (B4) will be differently distributed than those at larger scales such as (B5).

In theory the BDCs are only asymptotically scale similar. One has

$$a_{l;L} = \frac{W(i_1, \ldots, i_n) Z_N}{\frac{1}{2}(W(i_1, \ldots, i_{n-1}) Z_N + W'(i_1, \ldots, i_{n-1}) Z_N')} \qquad \text{(B6)}$$

where Z_N are the dressing factors equal to

$$Z_N = 2^{-N} \sum_{i_1,\ldots,i_N} W(i_1) W(i_1,i_2) \ldots W(i_1,\ldots,i_N), \qquad \text{(B7)}$$

and $Z_N \rightarrow Z_\infty$ for large N (as N increases Z_N, becomes a very narrow distributed variable).

In practice what is observed is that as one further increases the scale, the BDCs become more similarly distributed and after about 6 steps of dressing the BDC densities converge (visually) to the same curve for all subsequent steps of the breakdown. This means that on a visual basis canonical cascades which have been iterated at least 6 steps, or more, beyond the final scale and dressed back up to the final scale will seem scale similar on all scales.

Acknowledgments. The authors would like to thank C. D. Stow for use of the electronic gauges, as well as Kim Dirks and Roger Nathan who helped collect the data. The large scale C-band radar data used was kindly supplied by the New Zealand Meteorological Service and the authors thank Warren Gray of the National Institute of Water and Atmospheric Research (NIWA) for assistance in processing the Met Service radar data. Much thanks to Rebecca Godfrey for the final edits. Finally the authors thank the anonymous reviewers for their suggestions which led to an improved paper.

References

Davis, A., Marshak, A., Wiscombe, W., and Cahalan, R., Multifractal characterizations of nonstationarity and intermittency in geophysical fields: Observed, retrieved, or simulated, *J. Geophys. Res., 99(D4)*, 8055-8072, 1994.

Devroye, L., *Non-Uniform Random Variate Generation*, 843 pp., Springer-Verlag, New York, 1986.

Duncan, M. R., The Universal Multifractal Nature of Radar Echo Fluctuations, PhD Thesis, McGill University, Montreal, Canada, 1993.

Feller, *An Introduction to Probability Theory and its Applications, Volume II*, 626 pp., John Wiley & Sons, New York, 1966.

Foufoula-Georgiou, E., and Krajewski, W., Recent advances in rainfall modeling, estimation and forecasting, U.S. Natl. Rep. Int. Union Geod. Geophys: 1991-1994, *Rev. Geophys.*, 1125-1137, 1995.

Georgakakos, K. P., Carsteanu, A. A., Sturdevant, P. L., and Cramer, J. A., Observation and analysis of midwestern rain rates, *J. Appl. Meteorol., 33*, 1433-1444, 1994.

Gupta, V. K., and Waymire, E., Multiscaling properties of spatial rainfall and river flow distributions, *J. Geophys. Res., 95(D3)*, 1999-2009, 1990.

Gupta, V. K., and Waymire, E., A statistical analysis of mesoscale rainfall as a random cascade, *J. Appl. Meteor., 32*, 251-267, 1993.

Harris, D., Menabde, M., Seed, A. W., and Austin, G. L., Multifractal characterization of rain fields with a strong orographic influence, *J. Geophys. Res., 101(D21)*, 26 405-26 414, 1996.

Harris, D., Seed, A. W., Menabde, M., and Austin, G. L., Factors affecting multiscaling analysis of rainfall time series, *Nonlinear Proc. Geophysics, 4(3)*, 137-156, 1997.

Kahane, J. P., and Peyriere, J., Sur Certaines Martingales de Benoit Mandelbrot, *Adv. Math., 22*, 131-145, 1976.

Kida, S., Log-stable distribution and intermittency of turbulence, *J. Phys. Soc. Jap., 60(1)*, 5-8, 1991.

Lavallée, D., Lovejoy, S., Schertzer, D., and Ladoy, P., Nonlinear variability of landscape topography: Multifractal analysis and simulation, in *Fractals in Geography*, edited by Lam, N., and De Cola, L., pp.158-192, Prentice Hall, 1993.

Lovejoy, S., and Schertzer, D., Multifractals and rain, in *New Uncertainty Concepts in Hydrology and Water Resources*, edited by Kundzewicz, A. W., pp. 61-103, Cambridge Univ. Press, New York, 1995.

Marshak, A., Davis, A., Cahalan, R., and Wiscombe, W., Bounded cascade models as nonstationary multifractals, *Phys. Rev. E, 49(1)*, 55-59, 1994.

Menabde, M., Seed, A. W., Harris, D., and Austin, G. L., Self-similar random fields and rainfall simulation, *J. Geophys. Res., 102(D12)*, 13509-13515, 1997a.

Menabde, M., Harris, D., Seed, A. W., Austin, G. L., and Stow, C. D., Multiscaling properties of rainfall and bounded random cascades, *Water Resour. Res., 33(12)*, 2823-2830, 1997b.

Novikov, E. A., The effects of intermittency on statistical characteristics of turbulence and scale similarity of breakdown coefficients, *Phys. Fluids A, 2(5)*, 814-820, 1990.

Novikov, E. A., Infinitely divisible distributions in turbulence, *Phys. Rev. E, 50(5)*, R3303-R3305, 1994.

Pecknold, S., Lovejoy, S., Schertzer, D., Hooge, C., and Malouin, J. F., The simulation of universal multifractals, in *Cellular Automata: Prospects in Astrophysical Applications*, edited by Perdang, J. M., and Lejeune, A., pp. 228-267, World Sci., River Edge, New Jersey, 1993.

Pedrizzetti, G., Novikov, E. A., Praskovsky, A. A., Self-similarity and probability distributions of turbulent intermittency, *Phys. Rev. E, 53(1)*, 475-484, 1996.

Press, W. H., Teukolsky, S. A., Vetterling, W. T., Flannery, B. P., *Numerical Recipes in C. The Art of Scientific Computing. Second Edition*, Cambridge University Press, 1992.

Samorodnitsky, G., Taqqu, M. S., *Stable Non-Gaussian Random Processes: Stochastic Models with Infinite Variance*, Chapman & Hall, New York, New York, 1994.

Schertzer, D., and Lovejoy, S., Physical modeling and analysis of rain and clouds by anisotropic scaling multiplicative processes, *J. Geophys. Res, 92(D8)*, 9693-9714, 1987.

Spiegel, M. R., *Schaum's Outline of Theory and Problems of Statistics in SI Units, SI edition*, 359 pp., McGraw-Hill, New York, 1972.

Vainshtein, S. I., Sreenivasan, K. R., Pierrehumbert, R. T., Kashyap, V., and Juneja, A., Scaling exponents for turbulence and other random processes and their relationships with multifractal structure, *Phys. Rev. E, 50(3)*, 1823-1835, 1994.